Iraqi Journal of Science, 2024, Vol. 65, No .4, pp: 2065-2073
DOI: 10.24996/ijs.2024.65.4.24

ISSN: 0067-2904

Analysis of the Effect of Peristaltic Transport Flux on Channel Wall: Bingham Fluid as A Model

Dheia G. Salih Al-Khafajy, [2]Fathi Ali M Bribesh, [1]Mary Ghadbaan Thoubaan
[1] *Department of Mathematics, College of Science, University of Al-Qadisiyah, Diwaniya, Iraq*
[2]*Department of Mathematics, Faculty of Sciences, University of Zawia, Zawia, Libya*

Received: 13/4/2022 Accepted: 14/4/2023 Published: 30/4/2024

Abstract
This study is concerned with analyzing the peristaltic flow of Bingham fluid through an irregular tube with a short wavelength “relative to channel width” and using the governing equations of Bingham fluid in the Navier-Stokes equations in the Cartesian coordinate system. Significant results of the problem were obtained and analyzed using the Wolfram-Mathematica Computational Notebook.

Keywords: Bingham fluid, Peristaltic flow, Irregular flow channel**.**

تحليل تأثير تدفق النقل التمعجي على جدار القناة: سائل بينغهام كنموذج

ضياء غازي ، فتحي علي ، ماري غضبان
[1]قسم الرياضيات، كلية العلوم، جامعة القادسية، الديوانية، العراق
[2]قسم الرياضيات، كلية العلوم، جامعة الزاوية، الزاوية، ليبيا

الخلاصة
تهتم هذه الدراسة بتحليل التدفق التمعجي لمائع بينغهام من خلال قناة غير منتظمة، بافتراض طول موجي قصير جدًا "بالنسبة لعرض القناة" واستخدام المعادلات التي تحكم مائع بينغهام في معادلات نافيير–ستوكس في نظام الإحداثيات الديكارتية. حصلنا على نتائج مهمة للمسألة وتم تحليلها باستخدام برنامج Mathematica.

1. Introduction

The peristaltic flow of fluids is generated by the constriction and relaxation of the flow channel. It is widely used in the nuclear industry, as well as in the pattern of food ingestion through the esophagus, the movement of chyme in the digestive tract, the movement of small blood vessels such as veins, capillaries, arterioles, the flow of transporting urine from the kidneys to the bladder, transporting healthy fluids, transporting Corrosive liquids, and toxic liquids flow [1]. Latham [2] introduced the idea of fluid transport using peristaltic waves in mechanical and physiological studies. Subsequently, many other others have studied the mechanism of peristalsis due to the enormous importance of peristaltic flows in engineering and biomedicine. Others obtained various results regarding peristaltic flows in different types

*Email: dheia.salih@qu.edu.iq

of fluids through different flow channels. Shapiro [3] discussed pumping and reverse propagation of peristaltic waves. Yin and Fung followed it up [4], with an experimental study of peristaltic flow. Lakshminarayana, et al. [5] studied the effect of heating on the peristaltic sliding flow of Bingham's fluid in an oblique canal. While Vaidya, et al. [6] as an application of blood flow through narrowed arteries: studied Bingham's fluid flow with peristaltic effect with multiple chemical reactions. Almusawi and Abdulhadi [7] discussed the effect of heat transfer and dynamics in addition to circulation on the peristaltic transport of the irrigation fluid. Al-Khafajy and Al-Khalidi [8] considered the peristaltic flow of Jeffrey's fluid through an flexible tube. Al-Khafajy and Al-Delfi [9] presented a model of the peristaltic flow of Williamson's fluid through an elastic conduit. Recently, many studies analyzed the peristaltic flow of a Bingham fluid through different flow channel geometries, see for details [10], [11], [12], [13], [14], [15], [16], [17].

These studies had an impact on our choice of this subject to analyze the peristaltic flow of Bingham fluid through a channel in the form of a regular sine wave in Cartesian coordinates, which is a model close to the movement of blood in the arteries and veins of the human body.

2. Mathematical Formulations

We consider the peristaltic flow of Bingham fluid through an irregular channel. Where the equation of the flow channel boundary is in the form of the sine wave $\left(d_1 - \bar{\emptyset}\, sin^2\left(\frac{\pi}{\omega}(\bar{X} - s\bar{t})\right)\right)$ in the Cartesian coordinate system, where d_1 is the average radius of the tube, $\bar{\emptyset}$ is the amplitude of a peristaltic wave, ω is the wavelength, s is a wave propagation speed, and $\bar{t}$ is the time, see Figure 1. The geometry of the wall surface is described as:

$$H(\bar{x},\bar{t}) = d_1 - \bar{\emptyset}\, sin^2\left(\frac{\pi}{\omega}(\bar{x} - s\bar{t})\right)$$

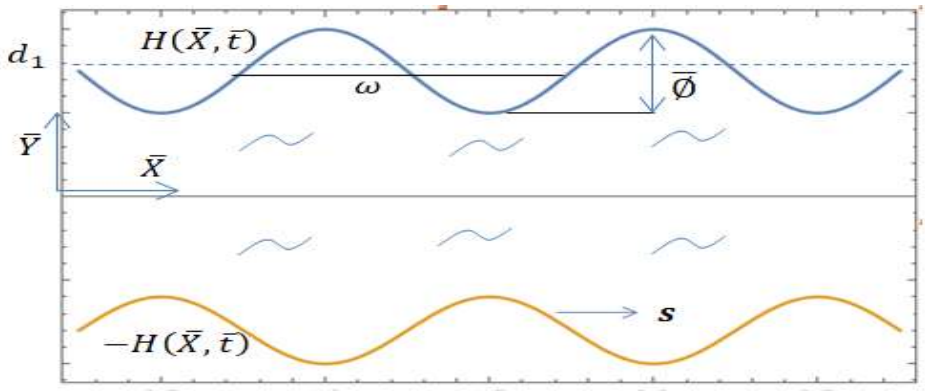

Figure 1: The Problem Geometry

Governing Equations

The basic governing equations of the continuity and the Navier-Stokes equations are

$\nabla.\bar{\mho} = 0$ (The continuity equation)

$\rho(\bar{\mho}.\nabla)\bar{\mho} = -\nabla\bar{P} + div\,\bar{\mathcal{S}}$ (Momentum equation)

where $\mho \equiv (U_1(X,Y,t), U_2(X,Y,t), 0)$ is a velocity field, ρ is a density, $\bar{P}$ is a pressure, and $\bar{\mathcal{S}}$ is an extra stress tensor.

The fundamental equation for the Bingham fluid is given by [5];

$$\bar{S} = \begin{cases} \mu\bar{\mathcal{X}} + \dfrac{\tau_1}{\bar{\dot{\gamma}}}\bar{\mathcal{X}} & \text{for} \quad \tau \geq \tau_1 \\ 0 & \text{for} \quad \tau < \tau_1, \end{cases}$$

where τ_1 is the yield stress, $\bar{\dot{\gamma}}$ is the shear rate, and $\bar{\mathcal{X}}$ the Rivlin-Ericksen tensors defined by $\bar{\mathcal{X}} = \nabla\bar{\mathcal{U}} + (\nabla\bar{\mathcal{U}})^T$, where $\nabla\bar{\mathcal{U}}$ is the velocity gradient, and $(\nabla\bar{\mathcal{U}})^{\mathrm{T}}$ is the transpose of the velocity gradient. However, $\dot{\gamma}$ is defined as

$$\dot{\gamma} = \sqrt{\frac{1}{2}\sum_i\sum_j \dot{\gamma}_{ij}\dot{\gamma}_{ji}} = \sqrt{2\left\{\left(\frac{\partial\overline{U_1}}{\partial\bar{X}}\right)^2 + \left(\frac{\partial\overline{U_2}}{\partial\bar{Y}}\right)^2\right\} + \left(\frac{\partial\overline{U_1}}{\partial\bar{Y}} + \frac{\partial\overline{U_2}}{\partial\bar{X}}\right)^2}.$$

Peristaltic motion is a normally unsteady phenomenon and it is possible to get the steady-state by reference assumption (by converting constant formulas) from the test frame $(\bar{X}, \bar{Y})$ to the wave frame $(\bar{x}, \bar{y})$ with the following relations

$$\left.\begin{aligned} (\bar{x}, \bar{y}) = (\bar{X} - s\bar{t}, \bar{Y}), \qquad \bar{p}(\bar{x}, \bar{y}) = \bar{P}(\bar{X} - s\bar{t}, \bar{Y}, \bar{t}), \\ (\overline{u_1}(\bar{x}, \bar{y}), \overline{u_2}(\bar{x}, \bar{y}), 0) = (\overline{U_1}(\bar{X} - s\bar{t}, \bar{Y}, \bar{t}) - s, \overline{U_2}(\bar{X} - s\bar{t}, \bar{Y}, \bar{t}), 0), \end{aligned}\right\} \tag{1}$$

where $(\overline{u_1}, \overline{u_2})$ and $(\overline{U_1}, \overline{U_2})$ are velocity elements of the moving and stationary structures. With these transformations, the equations of continuity and momentum, respectively, become

$$\frac{\partial(\overline{u_1} + s)}{\partial\bar{x}} + \frac{\partial\overline{u_2}}{\partial\bar{y}} = 0, \tag{2}$$

$$\left.\begin{aligned} \rho(\overline{u_1} + s)\frac{\partial(\overline{u_1} + s)}{\partial\bar{x}} + \rho\overline{u_2}\frac{\partial\overline{u_2}}{\partial\bar{y}} - \frac{\partial\bar{S}_{\bar{x}\bar{x}}}{\partial\bar{x}} - \frac{\partial\bar{S}_{\bar{x}\bar{y}}}{\partial\bar{y}} + \frac{\partial\bar{p}}{\partial\bar{x}} = 0, \\ \rho(\overline{u_1} + s)\frac{\partial\overline{u_2}}{\partial\bar{x}} + \rho\overline{u_2}\frac{\partial\overline{u_2}}{\partial\bar{y}} - \frac{\partial\bar{S}_{\bar{x}\bar{y}}}{\partial\bar{x}} - \frac{\partial\bar{S}_{\bar{y}\bar{y}}}{\partial\bar{y}} + \frac{\partial\bar{p}}{\partial\bar{y}} = 0, \end{aligned}\right\} \tag{3}$$

and the boundary conditions

$$\left.\begin{aligned} \overline{U_1} = 0 \ \text{ at } \ \bar{Y} = \pm H(\bar{x}) = \pm\left(d_1 - \bar{\emptyset}\, sin^2\left(\frac{\pi}{\omega}(\bar{X} - s\bar{t})\right)\right), \\ \overline{U_2} = 0 \ \text{ at } \ \bar{Y} = d_1 - \bar{\emptyset}\, sin^2\left(\frac{\pi}{\omega}(\bar{X} - s\bar{t})\right). \end{aligned}\right\} \tag{4}$$

The stress components are given by

$$\left.\begin{aligned} \bar{S}_{\bar{x}\bar{x}} = 2\left(\mu + \frac{\tau_1}{\bar{\dot{\gamma}}}\right)\frac{\partial\overline{u_1}}{\partial\bar{x}}, \quad \bar{S}_{\bar{y}\bar{y}} = 2\left(\mu + \frac{\tau_1}{\bar{\dot{\gamma}}}\right)\frac{\partial\overline{u_2}}{\partial\bar{y}}, \\ \bar{S}_{\bar{x}\bar{y}} = \bar{S}_{\bar{y}\bar{x}} = \left(\mu + \frac{\tau_1}{\bar{\dot{\gamma}}}\right)\left(\frac{\partial\overline{u_1}}{\partial\bar{y}} + \frac{\partial\overline{u_2}}{\partial\bar{x}}\right), \end{aligned}\right\} \tag{5}$$

and

$$\bar{\dot{\gamma}} = \sqrt{2\left\{\left(\frac{\partial\overline{u_1}}{\partial\bar{x}}\right)^2 + \left(\frac{\partial\overline{u_2}}{\partial\bar{y}}\right)^2\right\} + \left(\frac{\partial\overline{u_1}}{\partial\bar{y}} + \frac{\partial\overline{u_2}}{\partial\bar{x}}\right)^2}. \tag{6}$$

The corresponding stream functions are $\overline{u_1} = \frac{\partial\bar{\Psi}}{\partial y}$ and $\overline{u_2} = -\frac{\partial\bar{\Psi}}{\partial x}$.

Solution Method

In order to simplify the governing equations of the problem, we may introduce the following dimensionless transformations:

$$\left.\begin{aligned} x = \frac{\bar{x}}{\omega}, y = \frac{\bar{y}}{d_1}, \delta = \frac{d_1}{\omega}, u_1 = \frac{\overline{u_1}}{s}, u_2 = \frac{\omega\overline{u_2}}{sd_1}, p = \frac{{d_1}^2\bar{p}}{\mu\omega s}, t = \frac{s\bar{t}}{\omega}, \\ B = \frac{d_1\tau_1}{s\mu}, \Psi = \frac{\bar{\Psi}}{d_1 s}, \emptyset = \frac{\bar{\emptyset}}{d_1}, h = \frac{H}{d_1}, R_e = \frac{\rho s d_1}{\mu}, Q_1 = \frac{\overline{Q_1}}{d_1 s}, \\ q_1 = \frac{\overline{q_1}}{d_1 s}, \dot{\gamma} = \frac{d_1\,\bar{\dot{\gamma}}}{s}, \mathcal{S}_{xx} = \frac{\omega\,\bar{S}_{\bar{x}\bar{x}}}{\mu s}, \mathcal{S}_{xy} = \frac{d_1\,\bar{S}_{\bar{x}\bar{y}}}{\mu s}, \mathcal{S}_{yy} = \frac{\omega\,\bar{S}_{\bar{y}\bar{y}}}{\mu s} \end{aligned}\right\} \tag{7}$$

where Re is Reynolds number, B Bingham number, $\emptyset$ amplitude ratio, δ dimensionless wave number, and Ψ is the stream function. Substituting equations (7) into equations (2)-(6) under the long-wavelength assumption ($\delta \ll 1$), the governing equations after simplification become

$$\frac{\partial u_1}{\partial x} + \frac{\partial u_2}{\partial y} = 0. \tag{8}$$

$$\frac{\partial p}{\partial x} = \frac{\partial S_{xy}}{\partial y}. \tag{9}$$

$$\frac{\partial p}{\partial y} = 0, \tag{10}$$

and

$$S_{xy} = \frac{\partial u_1}{\partial y} + B, \tag{11}$$

with the boundary conditions:

$$\left.\begin{aligned} u_1(y) = u_1(-y) = -1 \text{ at } y = h = 1 - \emptyset\, sin^2(\pi x), \\ u_2(y) = 0 \text{ at } y = h = 1 - \emptyset\, sin^2(\pi x). \end{aligned}\right\} \tag{12}$$

Rate of Volume Flow

The instantaneous volume flow rate in a fixed coordinate system is given by

$$\widehat{Q_1} = \int_{-H}^{\bar{H}} \overline{U_1}(\bar{X}, \bar{Y}, \bar{t})\, d\bar{Y} \tag{13}$$

Substituting equations (1) into (13) and then integrating yields

$$\widehat{Q_1} = \overline{q_1} + 2sH,$$

where

$\overline{q_1} = \int_{-H}^{H} \overline{u_1}(\bar{x}, \bar{y})\, d\bar{y}$.

The time-mean flow over a period $T = \frac{\omega}{s}$ defined as

$$\overline{Q_1} = \frac{1}{T}\int_0^T \widehat{Q_1}\, d\bar{t} = \frac{1}{T}\int_0^T (\overline{q_1} + 2sH)\, d\bar{t} = \overline{q_1} + 2s\left(d_1 - \frac{\overline{\emptyset}}{2}\right).$$

By using equation (7), one obtains $Q_1 = q_1 + 2 - \emptyset$, thus $q_1 = Q_1 + \emptyset - 2$, where q_1 is the dimensionless volume flow rate in the wave frame defined by

$$q_1 = \int_{-h}^{h} u_1(x, y)\, dy = \int_{-h}^{h} \left(\frac{\partial \Psi}{\partial y}\right) dy = \Psi\big(h(x)\big) - \Psi\big(-h(x)\big).$$

We can find the stream function Ψ, by using the relationship $\Psi = \int u_1(x, y)\, dy$ and the boundary conditions:

$\left.\frac{\partial \Psi}{\partial y}\right|_{y=h} = \left.\frac{\partial \Psi}{\partial y}\right|_{y=-h} = -1, \qquad \Psi(h) = \frac{1}{2}q_1, \Psi(-h) = -\frac{1}{2}q_1.$

Solution of the Problem

Substituting equation (11) into equation (9) and using the boundary conditions (12) and volume flow rate q_1, we get the solution of the velocity equation. Therefore, the formula for the velocity function is

$u_1 = \frac{1}{2}\frac{\partial p}{\partial x}(y^2 - h^2) - 1,$

The corresponding stream function is

$\Psi = \frac{1}{2}\frac{\partial p}{\partial x}\left(\frac{1}{3}y^3 - h^2 y\right) - y,$

The shear stresses
$\mathcal{S}_{xy} = \frac{\partial p}{\partial x} y + B,$
where the evaluated pressure gradient is introduced as
$\frac{\partial p}{\partial x} = \frac{-3}{2h^3}(Q_1 + \emptyset - 2 + 2h).$
Integrating $\frac{\partial p}{\partial x}$ with respect to x per wavelength, we get pressure rise ΔP. The dimensionless friction force $\mathcal{J}$ at the wall per wavelength is given by
$\mathcal{J} = -\int_0^1 h^2 \left(\frac{\partial p}{\partial x}\right) dx.$

3. Results and Discussion

We discuss and analyze the solutions obtained for the velocity, shear stress, pressure gradient, pressure rise, friction forces and stream function, through results obtained using Wolfram-Mathematica software. We note that the fluid velocity increases with increasing the amplitude ratio of the flow channel $\emptyset$ and volume flow rate parameter Q_1, while the fluid velocity decreases with the progress in the flow channel on the x-axis as shown in
Figure **2** to Figure 4, respectively.

As indicated in Figure 6 and Figure **5**, the shear stress increases at the lower wall of the flow channel while it turns in the middle of the channel to be decreased (adjacent to the upper wall of the channel) with increasing $\emptyset$ and Q_1, respectively. Conversely, for the effect of distance on the shear stress. In Figure 8, it is observed that with the increase in the parameter of Bingham B, the shear stress increases. Figure 7, shows a decrease in the stress at the bottom wall of the flow channel, at the middle of the channel, it turned to be increased next to the channel's top wall when the fluid moves on the x-axis.
Error! Reference source not found., shows an increase in the pressure gradient at the m iddle of the flow channel while it decreases near the wall under the influence of increasing $\emptyset$.
Error! Reference source not found., shows the effect of the volume flow rate parameter on the pressure gradient, where the gradient function decreases with increasing Q_1.

Figure 11, shows the effect of ΔP"pressure rise" with Q_1"flux" for different values $\emptyset$. We first notice that the relationship between the flux and ΔP is linear and decreasing. In addition, when the flux is positive and does not exceed 0.35, there is a direct relationship between ΔP and $\emptyset$. If the flux exceeds 0.35, the relationship reverses as ΔP decreases versus increasing $\emptyset$. We also note that at low values of Q_1 (less than 1), ΔP is positive (retrograde pumping), and when the value of Q_1 exceeds one, the ΔP turns negative (augmented region).

The effect of flux Q_1 on the friction forces at the two walls of the flow channel for different values $\emptyset$ is shown in Figure 12. Whereas, it is observed that the effect of the flux on the friction forces is similar on the two walls of the channel (upper F_u and lower F_l) because of the symmetric flow channel. Note that, the relationship between Q_1 and $\mathcal{J}$ is linearly increasing. In addition, when the flux is positive and does not exceed 0.35, there is an inverse relationship between $\emptyset$ and $\mathcal{J}$, however, when the flux is higher than 0.35, the relationship is direct between $\emptyset$ and $\mathcal{J}$, where $\mathcal{J}$ increases with increasing $\emptyset$. It is observed at low values of Q_1 (less than 1) that the friction forces are negative, and when the value of Q_1 exceeds one, the friction forces turn positive.

The closed flow lines of the bolus are formed thanks to the peristaltic movement of the wall of the flow channel that affects the fluid flow inside the channel. Figure 13. and Figure 14. display the effect of the two parameters $\emptyset$ and Q_1 on the bolus, where it is noticed by

increasing the parameter $\emptyset$ that a bracelet is generated in the middle of the channel when $\emptyset = 0.2$ and expands until it turns into a wave when $\emptyset = 0.55$, then a new bracelet is generated at the wall of the channel when $\emptyset = 0.6$. This bracelet grows until it disappears after it turns into a wave as it is shown in Figure 13. Finally, there is a similarity between the parameters $\emptyset$ and Q_1 in the effect on the stream function as configured in Figure 14. Bracelet-like is created in the middle of the channel when $Q_1 = 0.845$ and stretches until it turns into a wave when $Q_1 = 1.165$, then a new bracelet is created at the channel wall when $Q_1 = 1.53$. This bracelet grows until it disappears after turning into a wave at $Q_1 = 1.75$.

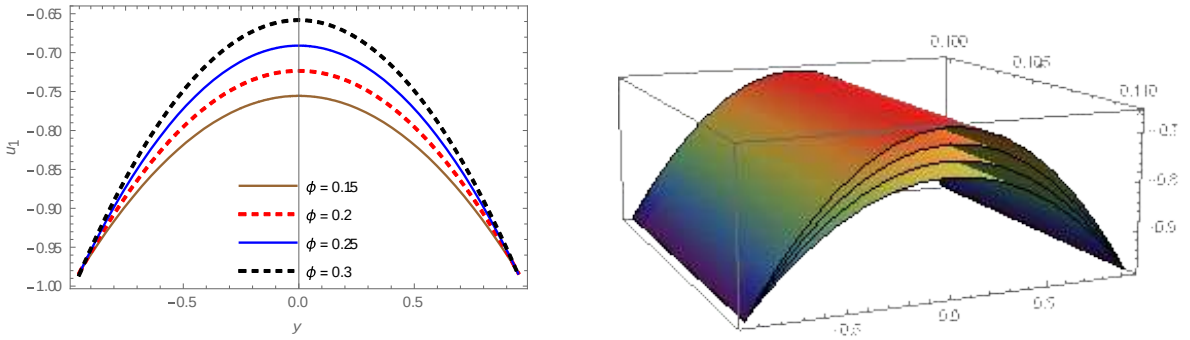

Figure 2: Velocity distribution for various values of $\emptyset$ with $Q_1 = 0.2$ and $x = 0.1$.

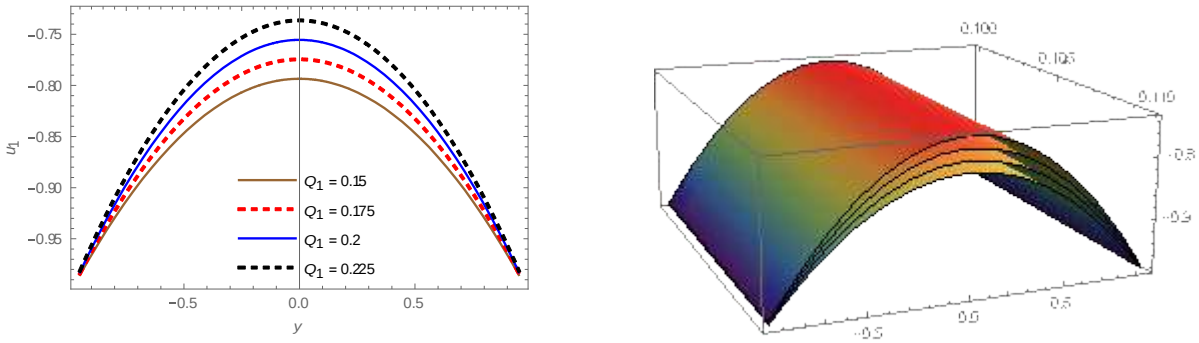

Figure 3: Velocity distribution for various values of Q_1 with $\emptyset = 0.15$ and $x = 0.1$.

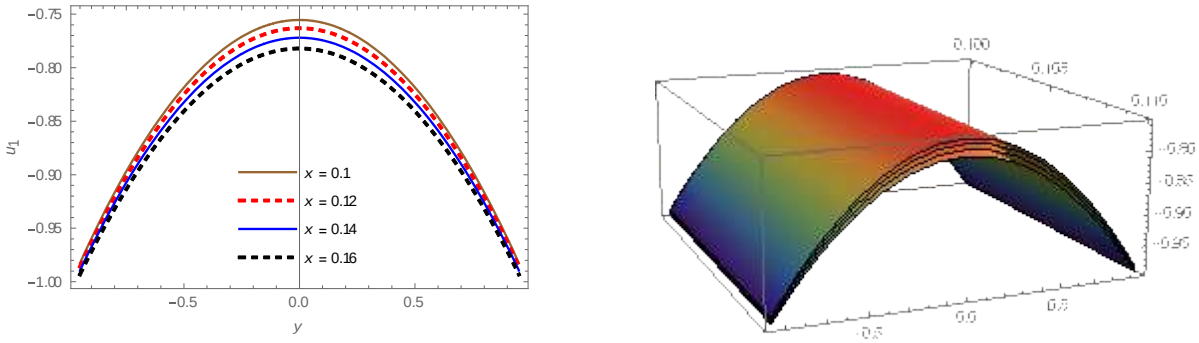

Figure 4: Velocity distribution for various values of x with $\emptyset = 0.15$ and $Q_1 = 0.2$.

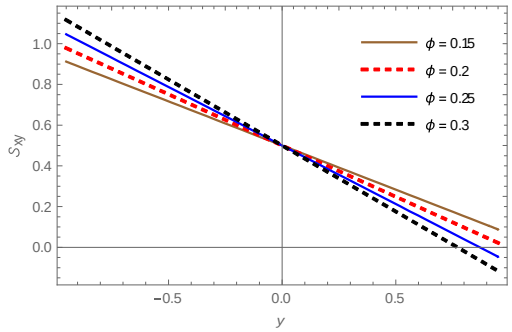

Figure 6: Shear stress profile for various values of $\emptyset$ with $Q_1 = 0.2$, $B = 0.5$, and $x = 0.1$.

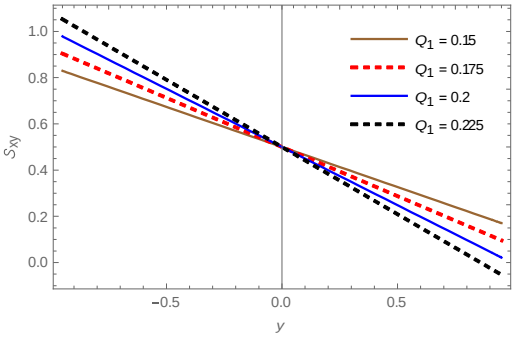

Figure 5: Shear stress profile for various values of Q_1 with $\emptyset = 0.15$, $B = 0.5$, and $x = 0.1$.

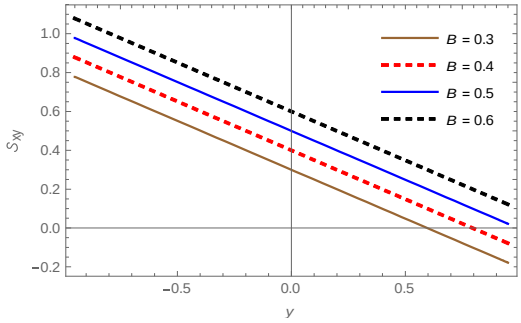

Figure 7: Shear stress profile for various values of B with $\emptyset = 0.15$, $Q_1 = 0.2$, and $x = 0.1$.

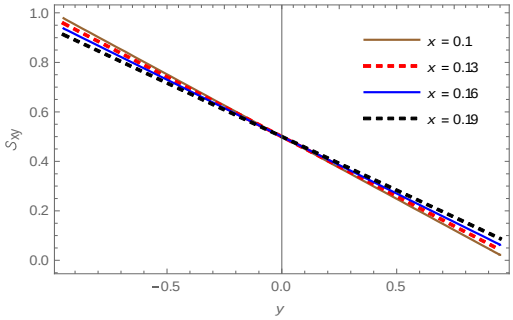

Figure 8: Shear stress profile for various values of x with $\emptyset = 0.15$, $Q_1 = 0.2$, and $B = 0.15$.

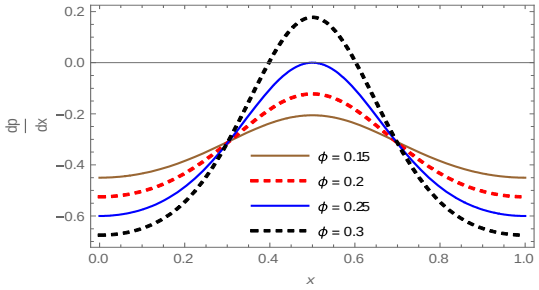

Figure 10: Pressure gradient distribution for various values of $\emptyset$ when $Q_1 = 0.2$

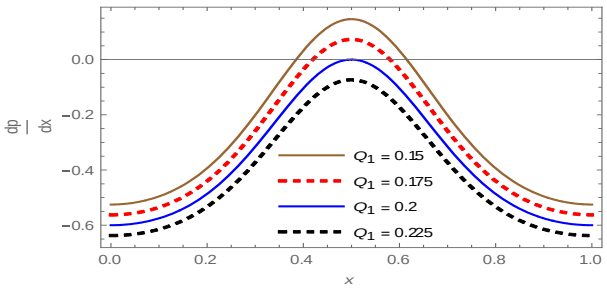

Figure 9: Pressure gradient distribution for various values of Q_1 when $\emptyset = 0.15$

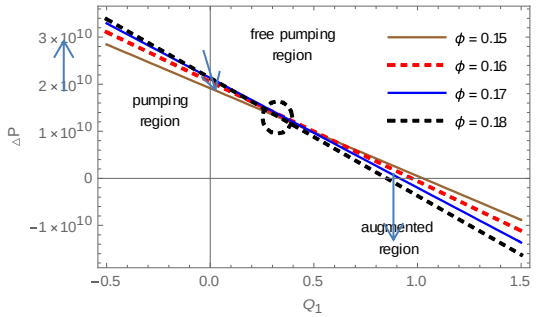

Figure 11: Pressure rise distribution with respect to Q_1 for various values of $\emptyset$.

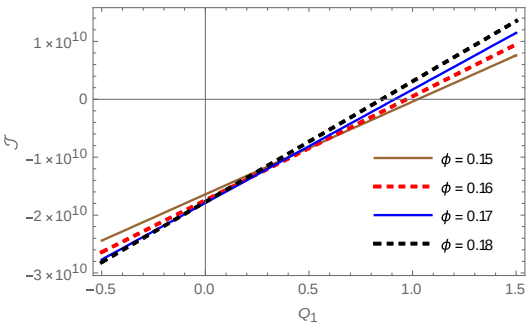

Figure 12: Frictional forces distribution with respect to Q_1 for various values of $\emptyset$.

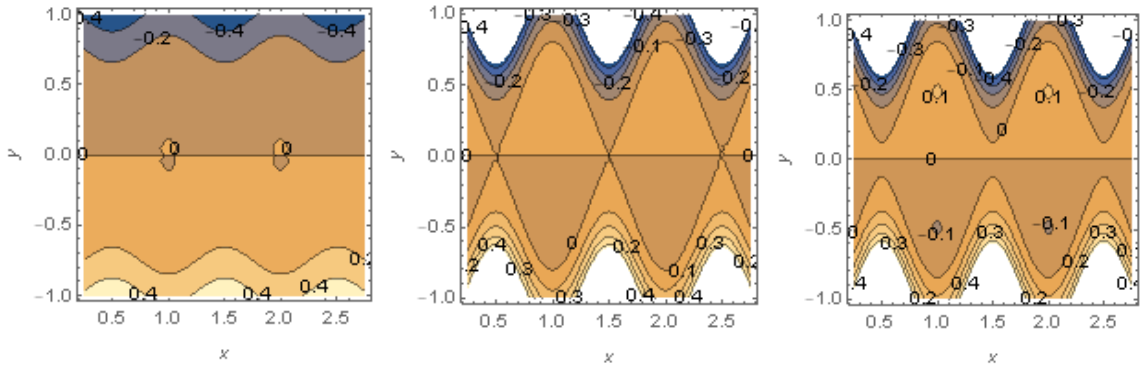

Figure 13: Wave frame streamlines for different values of $\phi = \{0.2, 0.5, 0.6\}$ when $Q_1 = 1.15$.

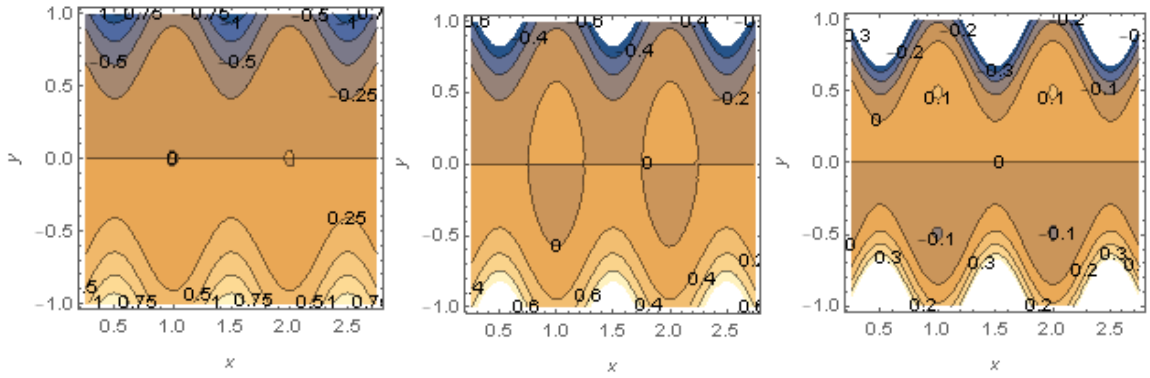

Figure 14: Wave frame streamlines for different values of $Q_1 = \{0.85, 1.165, 1.53\}$ when $\phi = 0.5$.

4. Concluding Remarks

Important results by studying the effect of the peristaltic flow of Bingham fluid through an irregular channel obtained, where the equation of the wall of the flow channel is in the form of a sine wave, which is a good analogy for the movement of blood through arteries and veins. Underneath, we briefly review some of the results we have drawn from this type of flow (peristaltic flow of blood through an artery) by the influence of two parameters "volume flow rate parameter Q_1 and capacitance ratio of flow channel $\emptyset$", these results are mostly consistent with similar studies for Bingham fluid with different channel geometry, see [10]-[17].

The velocity of blood through the circulation increases when Q_1 and $\emptyset$ are increased, respectively.

- Shear stress increases at the bottom artery wall and decreases at the upper wall with an effective increase of Q_1 and $\emptyset$, respectively.
- In the middle of the flow duct (artery) the pressure gradient increases with $\emptyset$ and decreases at the artery wall, while the pressure gradient decreases with increasing Q_1.
- The pressure rise is free ($\Delta P = 0$) when the flux $Q_1 = 0.35$ then the amplitude ratio of the flow channel $\emptyset$ has no effect on the pressure rise, and ΔP is positive (reflux pumping) when $Q_1$is less than 0.35 then the relationship between ΔP and $\emptyset$ is direct, and if Q_1 is more than 0.35 the inverse relationship between ΔP and $\emptyset$. Moreover, if Q_1exceeds 1, the ΔP will turn into negative (augmented zone).
- Frictional forces $\mathcal{J}$ are exactly opposite to the pressure rise under the influence of Q_1 and $\emptyset$.
- The effect of parameters $\emptyset$ and Q_1 on the stream function is the same, where a mid-channel bracelet is generated and expands until it turns into a wave, then a new bracelet is generated

near the channel wall and the bracelet expands until it disappears after being transformed into a wave for specific values of $\emptyset$ and Q_1 respectively.

References

[1] A. A. H. Al-Aridhee and D. G. S. Al-Khafajy, "Influence of MHD Peristaltic Transport for Jeffrey Fluid with Varying Temperature and Concentration through Porous Medium," in *Journal of Physics: Conference Series*, 2019.

[2] T. W. Latham, Fluid motions in a peristaltic pump., Massachusetts Institute of Technology, 1966.

[3] A. H. Shapiro, "Pumping and retrograde diffusion in peristaltic waves," in *Proc. Workshop Ureteral Reflux Children, Nat. Acad. Sci., Washington, DC*, 1967.

[4] F. C. P. Yin and Y. C. Fung, "Comparison of theory and experiment in peristaltic transport," *Journal of Fluid Mechanics*, vol. 47, no. 1, pp. 93-112, 1971.

[5] P. Lakshminarayana, K. Vajravelu, G. Sucharitha and S. Sreenadh, "Peristaltic slip flow of a Bingham fluid in an inclined porous conduit with Joule heating," *Applied Mathematics and Nonlinear Sciences*, vol. 3, no. 1, pp. 41-54, 2018.

[6] H. Vaidya, C. Rajashekhar, K. V. Prasad, S. U. Khan, F. Mebarek-Oudina, A. Patil and P. Nagathan, "Channel flow of MHD bingham fluid due to peristalsis with multiple chemical reactions: an application to blood flow through narrow arteries," *SN Applied Sciences*, vol. 3, pp. 1-12, 2021.

[7] B. A. Almusawi and A. M. Abdulhadi, "Heat Transfer Analysis and Magnetohydrodynamics Effect on Peristaltic Transport of Ree--Eyring Fluid in Rotating Frame," *Iraqi Journal of Science*, vol. 62, no. 8, pp. 2714-2725, 2021.

[8] D. G. S. Al-Khafajy and A. L. Noor, "The Peristaltic Flow of Jeffrey Fluid through a Flexible Channel," *Iraqi Journal of Science*, pp. 5476-5486, 2022.

[9] D. Al-Khafajy and W. N. Al-Delfi, "The Peristaltic Flow of Williamson Fluid through a Flexible Channel," *Iraqi Journal of Science*, pp. 865-877, 2023.

[10] M. Rafiq, A. Shaheen, Y. Trabelsi, S. M. Eldin, M. I. Khan and D. K. Suker, "Impact of activation energy and variable properties on peristaltic flow through porous wall channel," *Scientific Reports*, vol. 13, no. 1, p. 3219, 2023.

[11] L. Fusi and A. Farina, "Peristaltic flow of a Bingham fluid in a channel," *International Journal of Non-Linear Mechanics*, vol. 97, pp. 78-88, 2017.

[12] C. Rajashekhar, G. Manjunatha, F. Mebarek-Oudina, H. Vaidya, K. V. Prasad, K. Vajravelu and A. Wakif, "Magnetohydrodynamic peristaltic flow of Bingham fluid in a channel: An application to blood flow," *Journal of Mechanical Engineering and Sciences*, vol. 15, no. 2, pp. 8082-8094, 2021.

[13] R. Saravana, P. Hariprabakaran, R. Hemadri Reddy and S. Sreenadh, "Peristaltic Flow of a Bingham Fluid in Contact with a Jeffrey Fluid," in *Applications of Fluid Dynamics*, 2018.

[14] N. T. Eldabe, M. Abouzeid and H. A. Shawky, "MHD peristaltic transport of Bingham blood fluid with heat and mass transfer through a non-uniform channel," *Journal of Advanced Research in Fluid Mechanics and Thermal Sciences*, vol. 77, no. 2, pp. 145-159, 2021.

[15] A. M. Abd-Alla, S. M. Abo-Dahab, E. N. Thabet and M. A. Abdelhafez, "Impact of inclined magnetic field on peristaltic flow of blood fluid in an inclined asymmetric channel in the presence of heat and mass transfer," *Waves in Random and Complex Media*, pp. 1-25, 2022.

[16] U. R. Singh and U. Shanker, "Peristaltic Pumping of Bingham Plastic Fluid through a non-uniform Channel," *Int. J. of M Eng.*, vol. 7, no. 2, pp. 4408-4414, 2022.

[17] R. Choudhari, M. Gudekote, H. Vaidya, K. V. Prasad and S. U. Khan, "Rheological effects on peristaltic transport of Bingham fluid through an elastic tube with variable fluid properties and porous walls," *Heat Transfer*, vol. 49, no. 6, pp. 3391-3408, 2020.